

The present report attempted to show the clinicopathological features of completely resected colorectal PC compared with noncurative resected colorectal PC and to assess the rates and patterns of recurrence after macroscopically complete resection of colorectal PC. We attempted to determine the clinicopathological factors that predict specific patterns of recurrence, and we furthermore examined the clinicopathological features of patients surviving for 5 years with colorectal PC.

### PATIENTS AND METHODS

From January 1998 to December 2007, 153 patients were diagnosed with colorectal cancer including 4 appendiceal cancer and PC at the Wakayama Medical University Hospital (WMUH) and its related teaching hospitals, and 31 patients with macroscopically complete resections (R0, no residual tumor) were analyzed. No patients had received an extended cytoreductive operation or intraperitoneal hyperthermic chemotherapy described by Sugarbaker and Jablonski.<sup>3</sup> If the carcinomas were localized such as in the pelvic space, then we performed partial peritonectomy. 5-Fluorouracil (5-FU)-based chemotherapy was performed in patients of 80 years of age or younger and a performance status of less than 2 for 1 year. After tumor recurrence and noncompletely resected patients, modern systemic chemotherapy including IFL (bolus 5-FU+leucovorin+irinotecan, after 2000), FOLFIRI (bolus and infusional 5-FU+leucovorin+irinotecan, after 2005), and FOLFOX (bolus and infusional 5-FU+leucovorin+oxaliplatin, after 2005) was administered to patients who could tolerate these therapies. The administration of bevacizumab was introduced after 2007. Cetuximab was not available in Japan until 2009, and it therefore was not introduced in this study. Chemotherapy basically was performed until tumor progression. Preoperative enhanced chest and abdominal computed tomography (CT) was performed. We did not employ intraoperative hepatic ultrasound and positron emission tomography routinely. The patients underwent chest and abdominal CT and ultrasound every 4 months until 2 years postoperatively. From the third year onward, these examinations were performed every 6 months. Hematological testing including serum carcinoembryonic antigen (CEA) was performed every 4 months. An appropriate examination also was performed if the patients developed any symptoms.

The extent of PC was graded according to the following Japanese classification of colorectal carcinoma<sup>12</sup>: P1, metastases only to the adjacent

**Table I.** Patient characteristics

Age (y)	
Median	67
Range	16–92
Types of operation (No.)	
Right colectomy	48
Transverse colectomy	5
Left colectomy	37
Anterior resection	16
Hartmann	19
APR	1
Bypass	10
Stoma	17
Combined resected sites (No.)	
Liver	8
Small intestine	6
Large intestine	9
Ovary	14
Spleen	3
Urinary bladder	2
Uterus	5
Histopathologic types (No.)	
Well and Mod	101
Por	8
Muc	11
Sig	4
Pap	2
Not resected	27
Examined LN (No.)	
Mean ± SD	8.5 ± 5.7

APR, Abdominoperineal resection; LN, lymph nodes; Mod, moderately differentiated adenocarcinoma; Muc, mucinous adenocarcinoma; Pap, papillary adenocarcinoma; Por, poorly differentiated adenocarcinoma; SD, standard deviation; Sig, signet-ring cell carcinoma; Well, well-differentiated adenocarcinoma.

peritoneum that can be removed by a combined resection; P2, a few metastases to the distant peritoneum; and P3, numerous metastases to the distant peritoneum. In the present study, P1 was classified as limited PC because it can be macroscopically and completely resected with the primary lesion, whereas P2 and P3 were classified as extended PC because it is impossible to perform a complete resection in almost all cases.

Ten factors, including gender, age, location of tumor, histopathologic type, extent of PC, presence of extraperitoneal metastases, presence of regional lymph node (LN), and the depth of tumor invasion were evaluated as clinicopathological factors.

A statistical analysis was performed using the Stat-view J software program, version 5.0 (SAS Institute Inc., Cary, NC). Clinicopathological features between macroscopically complete resection and noncomplete resection were determined by

**Table II.** Clinicopathological features between macroscopically complete resection patients and noncomplete resection patients

Variables	Macroscopically complete resection		P value
	Yes (n = 31) No. of patients (%)	No (n = 122) No. of patients (%)	
Age (y)			.800
≥65 (n = 87)	17 (55)	70 (57)	
<65 (n = 66)	14 (45)	52 (43)	
Gender			.801
Male (n = 82)	16 (52)	66 (54)	
Female (n = 71)	15 (48)	56 (46)	
Location			.045
Colon (n = 115)	19 (61)	96 (79)	
Rectum (n = 38)	12 (39)	26 (21)	
Extraperitoneal metastases			<.001
Yes (n = 69)	4 (13)	65 (53)	
No (n = 84)	27 (87)	57 (47)	
Extent of PC			<.001
Limited (n = 60)	28 (90)	32 (26)	
Extended (n = 93)	3 (10)	90 (74)	
Preoperative CEA level			.329
>5 ng/mL (n = 103)	20 (65)	83 (68)	
≤5 ng/mL (n = 41)	11 (35)	30 (25)	
Unknown (n = 9)	0 (0)	9 (7)	
LN metastases			.039
Yes (n = 82)	17 (55)	65 (53)	
No (n = 36)	14 (45)	22 (18)	
Unknown or not excised (n = 35)	0 (0)	35 (29)	
Depth of tumor invasion			.675
≤T3 (n = 26)	6 (19)	20 (16)	
T4 (n = 97)	25 (81)	72 (59)	
Unknown of not excised (n = 30)	0 (0)	30 (25)	
Presence of ascites			.071
Yes (n = 67)	9 (29)	58 (48)	
No (n = 86)	22 (71)	64 (52)	
Histopathologic type			.272
Well and mod (n = 101)	25 (81)	76 (62)	
Others (n = 25)	6 (19)	19 (16)	
Not excised (n = 27)	0 (0)	27 (22)	

using the  $\chi^2$  analysis or Fisher's exact test. The cumulative overall and disease-free estimates were evaluated by the Kaplan-Meier method, and findings were compared for significance by the log-rank test. *P* values were calculated in all studies. This retrospective study was carried out according to the guidelines of the ethical committee of WMUH.

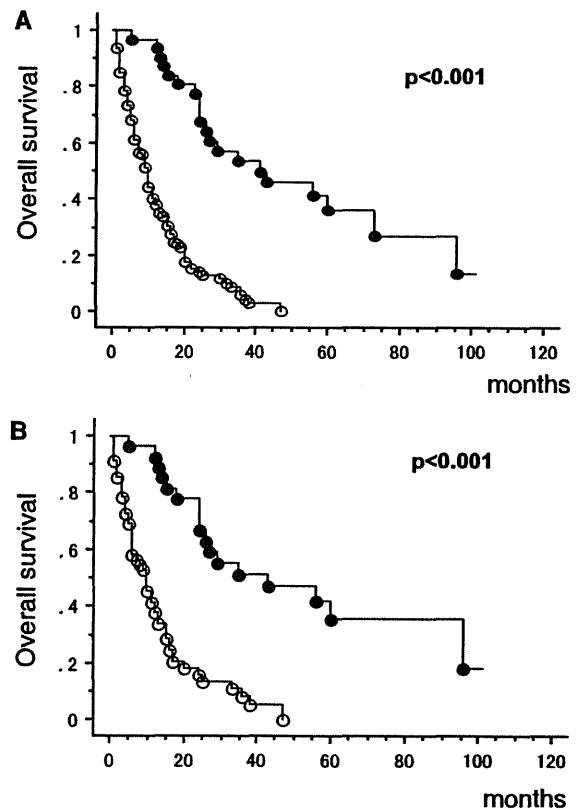


**Fig 1.** A, Cumulative survival curves of all patients measured from the time of the primary resection. The survival rate of patients of complete resection group (filled circles) was higher than that of patients in the noncomplete resection group (open circles) ( $P < .001$ ). B, Cumulative survival curves without cases with extraperitoneal metastases measured from the time of the primary resection. The survival rate of patients of complete resection group (filled circles) was also higher than that of patients in the noncomplete resection group (open circles) ( $P < .001$ ).

## RESULTS

**Clinicopathological features between macroscopically complete and noncomplete resection for colorectal PC.** The patient characteristics of the enrolled patients are summarized in Table I. We have shown the types of operations, combined resected sites, histopathologic types, and number of examined LN. Thirty-one of 153 patients (20.3%) with synchronous colorectal PC had received a macroscopically complete resection. Table II shows a comparison between complete and noncomplete resection for colorectal PC. No significant differences were found in age, gender, preoperative serum CEA level, depth of tumor, the presence of ascites, or histopathological type between the 2 groups. Significant differences were noted,

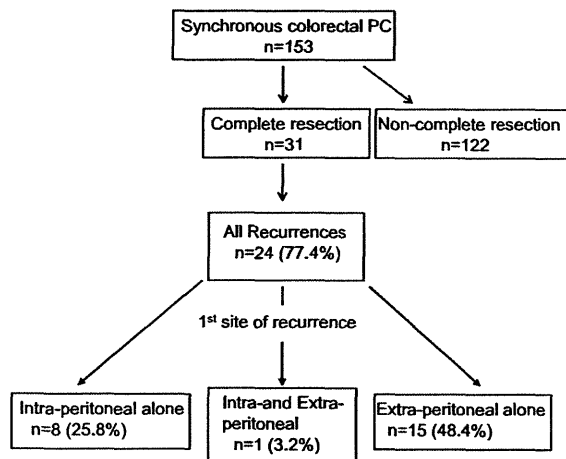


**Fig 2.** First pattern of recurrence. Twenty-four of 31 patients (77.4%) developed a tumor recurrence. Among all patients, 8 developed intraperitoneal disease as the first site of recurrence. One patient had intra- and extraperitoneal recurrence, and 15 had extraperitoneal disease alone.

however, in the primary tumor location, presence or absence of extraperitoneal metastases, extent of PC, and presence or absence of regional LN metastases ( $P = .045$ ,  $P < .001$ ,  $P < .001$ , and  $P = .039$ , respectively). Fig 1, A shows the overall patient survival curve from the time of the primary resection. The 5-year survival rate in the complete resection group was 36.0%, whereas that in the noncomplete group was 0% ( $P < .001$ ). When we excluded the patients with extraperitoneal metastases such as liver metastases, the clinical impact of a macroscopically complete resection also was shown ( $P < .001$ ) (Fig 1, B).

**Rates and patterns of recurrence.** Twenty-four of 31 patients (77.4%) who underwent a macroscopically complete resection had recurrent disease. Among all 24 patients with recurrence, 8 patients (25.8%) developed intraperitoneal disease alone as a first site of recurrence, 15 patients (48.4%) developed extraperitoneal disease alone, and 1 patient (3.2%) developed intra- and extraperitoneal recurrences (Fig 2). The 3- and 5-year intraperitoneal recurrence-free survival rates were 75.0% and 63.9%, respectively (Fig 3). The 3- and 5-year extraperitoneal recurrence free survival rates were 49.4% and 33.8%, respectively (Fig 4).

**Clinicopathological factors affecting the site of recurrence.** Although the presence of extraperitoneal metastases tended to be a worse indicator of intraperitoneal recurrence-free survival ( $P = .056$ ), no significant clinicopathological factors were associated with an increased risk of intraperitoneal recurrence (Table III). However, patients with

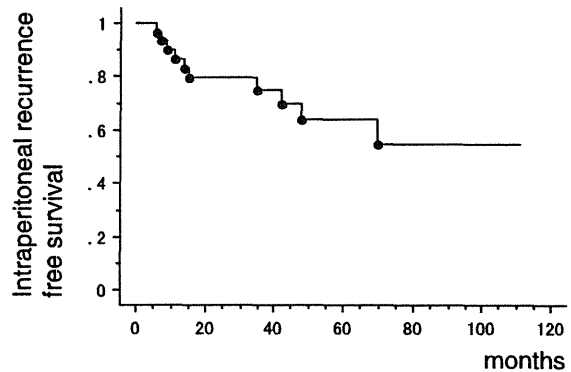


**Fig 3.** Intraperitoneal recurrence-free curves from the time of the resection in patients of colorectal peritoneal carcinomatosis. The 5-year intraperitoneal recurrence-free survival rate was 63.9%.

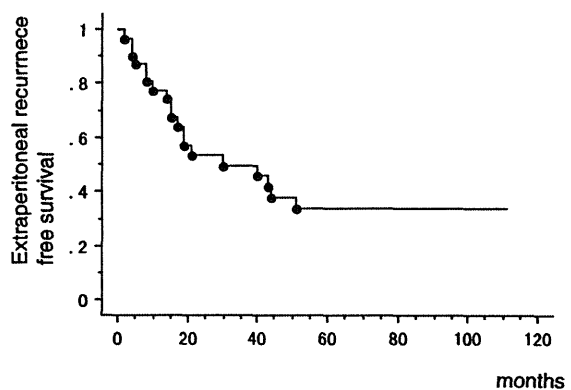


**Fig 4.** Extraperitoneal recurrence-free curves from the time of resection in patients with colorectal peritoneal carcinomatosis. The 5-year extraperitoneal recurrence-free survival rate was 33.8%.

extended PC ( $P = .009$ ) and presence of LN metastases ( $P = .023$ ) were associated with an increased risk of extraperitoneal metastases according to the univariate analysis. The T4 depth of tumor invasion tended to be a poor indicator of extraperitoneal recurrence-free survival, but it was not a statistically significant trend ( $P = .090$ ) (Table IV).

**Clinicopathological features of 5-year survivors.** Eleven of 31 patients survived for 5 years. Their status is listed in Table V. The extent of PCs of all patients was limited. Four of 11 patients had positive LN metastases. Four patients had recurrent disease, and 2 of these patients had received a hepatectomy against the liver metastases. Seven of these patients currently have a disease-free status. Three patients succumbed from recurrent disease, and 1 patient died of other causes.

**Table III.** Univariate analysis of clinicopathological factors affecting intraperitoneal recurrence-free patient survival after the complete resection of colorectal PC

Category	No. of patients (%)	3-year	5-year	P value
Gender				
Male	16 (52)	65.6	56.3	.565
Female	15 (48)	85.7	73.5	
Age				
<70	20 (65)	76.9	68.3	.539
≥70	11 (35)	72.7	54.5	
Location				
Colon	19 (61)	70.0	60.0	.927
Rectum	12 (39)	83.3	71.4	
Histopathologic type				
Well and mod	25 (81)	78.4	71.0	.178
Others	6 (19)	60.0	30.0	
Serum CEA level				
≤5 ng/mL	10 (35)	90.0	90.0	.146
>5 ng/mL	21 (65)	69.2	54.5	
Ascites				
Present	9 (29)	77.8	64.8	.667
Absent	22 (71)	73.1	64.0	
Extent of PC				
Limited	28 (90)	76.4	65.0	.431
Extended	3 (10)	66.7	66.7	
Extraperitoneal metastases				
Present	4 (13)	50.0	50.0	.056
Absent	27 (87)	78.8	66.1	
LN metastases				
Present	17 (55)	74.5	74.5	.914
Absent	14 (45)	76.2	57.1	
Depth of tumor invasion				
≤T3	6 (19)	80.0	80.0	.277
T4	25 (81)	75.6	59.5	

**Table IV.** Univariate analysis of clinicopathological factors affecting extraperitoneal recurrence-free patient survival after the complete resection of colorectal PC

Category	No. of patients (%)	3-year	5-year	P value
Gender				
Male	16 (52)	53.8	30.8	.881
Female	15 (48)	55.0	37.5	
Age				
<70	20 (65)	52.8	34.2	.602
≥70	11 (35)	43.6	32.7	
Location				
Colon	19 (61)	51.7	45.2	.427
Rectum	12 (39)	46.9	18.8	
Histopathologic type				
Well and mod	25 (81)	53.8	38.5	.408
Others	6 (19)	33.3	16.7	
Serum CEA level				
≤5 ng/mL	10 (35)	48.0	24.0	.279
>5 ng/mL	21 (65)	50.3	38.3	
Ascites				
Present	9 (29)	63.5	38.1	.419
Absent	22 (71)	44.1	33.0	
Extent of PC				
Limited	28 (90)	54.9	37.5	.009
Extended	3 (10)	0	0	
Extraperitoneal metastases				
Present	4 (13)	0	0	.419
Absent	27 (87)	54.9	37.5	
LN metastases				
Present	17 (55)	31.8	15.9	.023
Absent	14 (45)	70.1	54.5	
Depth of tumor invasion				
≤T3	6 (19)	83.3	62.5	.090
T4	25 (81)	40.3	25.2	

## DISCUSSION

Synchronous PC is observed in approximately 5–8% of patients with colorectal cancer as observed during the initial operation.<sup>1,2</sup> Although colorectal PC has been considered a preterminal cancer, several studies have reported the efficacy of cytoreductive operative therapy in combination with intraperitoneal chemotherapy in selected patients<sup>3–10</sup>; however, even after a complete resection of colorectal PC, most patients still develop recurrent disease.

First, we demonstrated the clinicopathological features of patients who underwent a macroscopically complete resection or an incomplete resection, and we also have shown the clinical impact of complete resection. According to our data, we should take into consideration the extended

peritonectomy if a macroscopical complete resection can be performed. The incidence of extraperitoneal metastases was low in the complete resection group, and the incidence of rectal primary location and no LN involvement was high in the complete resection group. The PCs originating from the rectum might not be likely to involve massive carcinomatosis because of its location. LN metastases might be a powerful marker, even in the status of PC.

The clinicopathological features of completely resected colorectal PCs have not been identified in previous reports.<sup>11</sup> A natural historical study reveals that the rate of metachronous PC was approximately 5%.<sup>2</sup> The 5-year incidence rate of intraperitoneal recurrence in the present study was 36.1%. The intraperitoneal recurrence rate was high, even after the complete resection of

**Table V.** Characteristics of 5-year survivors ( $n = 11$ )

Age/Sex	Extent of Pc	Location	Pathologic type	LN metastases	First recurrent site (time, months)	Follow-up (months)	Status
67/F	Limited	Rectum	Mod	Yes	LN (51)	96	DOD
50/F	Limited	Rectum	Well	Yes	Liver (30)	73	DOD
53/F	Limited	Rectum	Well	Yes	No	81	NED
78/M	Limited	Colon	Well	No	No	76	NED
69/F	Limited	Colon	Mod	No	No	111	NED
76/F	Limited	Colon	Well	Yes	No	68	NED
69/M	Limited	Colon	Muc	No	Liver (44)	63	NED
71/F	Limited	Colon	Well	No	No	64	DOO
39/F	Limited	Colon	Sig	No	Peritoneum (48)	60	DOD
50/M	Limited	Rectum	Mod	No	No	96	NED
55/M	Limited	Colon	Mod	No	No	71	NED

DOD, Dead of disease; NED, no evidence of disease; DOO, dead of other cause.

colorectal PC. Although no randomized controlled study has been conducted yet to show the efficacy of intraperitoneal chemotherapy for intraperitoneal recurrence after the resection of colorectal PC in the era of modern systemic chemotherapy, intraperitoneal chemotherapy may reduce the incidence of intraperitoneal recurrence rate.

Previous reports showed that the 5-year survival rate varied from 22% to 54% after the complete resection of colorectal PC.<sup>4,6-10</sup> The overall 5-year survival rate of the PC patients in our study was 36.0%. These findings show that synchronous PC is not necessarily preterminal, which is consistent with other data on resectable colorectal liver metastases.<sup>13,14</sup> In the present study, only 31 of 153 patients (20.3%) with synchronous colorectal PC had received a macroscopically complete resection, and 4 of 11 patients who survived for 5 years have undergone another reduction operation after tumor recurrence. We previously have reported the significance of repeat reduction operative therapy after the potentially curative resection of colorectal liver metastases,<sup>15</sup> and it is important to consider that repeat reduction operative therapy also may be useful for removing recurrent tumors, even after the resection of colorectal PC. In the field of colorectal liver metastases, it is important to identify the rates and patterns of recurrence after the resection of colorectal liver metastases.<sup>16,17</sup>

In the present study, we attempted to show the risk factor for intra- and extraperitoneal recurrence after a resection in patients with colorectal PC. No significant risk factors were noted for intraperitoneal recurrence. If we use several genetic and molecular markers, then we may show the risk factors of recurrence. In this study, the extent of PC was categorized by the Japanese classification criteria,<sup>12</sup> which identified 3

categories, rather than using the Peritoneal Cancer Index (PCI) as described by Jacquet and Sugarbaker.<sup>18</sup> The extent of PC in almost all patients who underwent a complete resection was limited, and we could not show any correlation between the extent of PC and intraperitoneal recurrence. If we adopt the PCI criteria, then we therefore may be able to identify those patients who are most likely to develop intraperitoneal recurrence. We should make use of the PCI criteria in the future studies. Positive LN metastases and extended PC, however, were the risk factors for extraperitoneal recurrences ( $P = .023$  and  $P = .009$ , respectively). This is the first report to show the risk factors of recurrence after macroscopically curative resection for colorectal PC. Although the histopathologic types of almost patients were well and moderately differentiated adenocarcinoma, the histopathological types were not the risk factor for recurrence. These results will help us to understand the patterns of recurrence and to direct the post-surgical treatment; however, this study had several limitations. This analysis was a retrospective study and consisted of a few patients. We could not perform a multivariate analysis because of the small number of patients. In the future, it is important to identify the risk factors for recurrence based on a large-scale cohort study.

In conclusion, we herein demonstrated the clinical impact of complete resection of colorectal PC while also showing the rates and patterns of recurrence after a macroscopically curative resection for colorectal PC.

#### REFERENCES

1. Japanese Society for Cancer of the Colon and Rectum. Multi-institutional registry of large bowel cancer in Japan. Vol. 28. Cases treated in 1999.

2. Jayne DG, Fook S, Loi C, Seow-Choen F. Peritoneal carcinomatosis from colorectal cancer. *Br J Surg* 2002;89:1545-50.
3. Sugarbaker PH, Jablonski KA. Prognostic features of 51 colorectal and 130 appendiceal cancer patients with peritoneal carcinomatosis treated by cytoreductive surgery and intraperitoneal chemotherapy. *Ann Surg* 1995;221:124-32.
4. Glehen O, Kwiatkowski F, Sugarbaker PH, Elias D, Levine EA, Simone M, et al. Cytoreductive surgery combined with perioperative intraperitoneal chemotherapy for the management of peritoneal carcinomatosis from colorectal cancer: a multi-institutional study. *J Clin Oncol* 2004;22:3284-92.
5. Verwaal VJ, Ruth S, Bree E, Slooten GW, Tinterenz H, Boot H, et al. Randomized trial of cytoreduction and hyperthermic intraperitoneal chemotherapy versus systemic chemotherapy and palliative surgery in patients with peritoneal carcinomatosis of colorectal cancer. *J Clin Oncol* 2003;21:3727-43.
6. Elias D, Gilly F, Boutitie F, Quenet F, Bereder JM, Mansvelt B, et al. Peritoneal colorectal carcinomatosis treated with surgery and perioperative intraperitoneal chemotherapy: retrospective analysis of 523 patients from a multicentric French study. *J Clin Oncol* 2010;28:63-8.
7. Shen P, Hawksworth J, Lovato J, Loggie BW, Geisinger KR, Fleming RA, et al. Cytoreductive surgery and intraperitoneal hyperthermic chemotherapy with mitomycin C for peritoneal carcinomatosis from nonappendiceal colorectal carcinoma. *Ann Surg Oncol* 2004;11:178-86.
8. Culliford AT, Brooks AD, Sharma S, Saltz LB, Schwartz GK, O'Reilly EM, et al. Surgical debulking and intraperitoneal chemotherapy for established peritoneal metastases from colon and appendix cancer. *Ann Surg Oncol* 2004;8:787-95.
9. Glehen O, Cotte E, Schreiber V, Sayag-Beaujard AC, Vignal J, Gilly FN. Intraperitoneal chemohyperthermia and attempted cytoreductive surgery in patients with peritoneal carcinomatosis of colorectal origin. *Br J Surg* 2004;91:747-54.
10. Verwaal VJ, Ruth S, Witkamp A, Boot H, Slooten G, Zoetmulder FAN. Long-term survival of colorectal carcinomatosis of colorectal origin. *Ann Surg Oncol* 2005;12:65-71.
11. Verwaal VJ, Boot H, Aleman BMP, Tinterenz H, Zoetmulder FAN. Recurrence after peritoneal carcinomatosis of colorectal origin treated by cytoreduction and hyperthermic intraperitoneal chemotherapy: location, treatment, and outcome. *Ann Surg Oncol* 2004;11:375-9.
12. Japanese Society for Cancer of the Colon and Rectum. Japanese classification of colorectal carcinoma. 2nd ed. Tokyo, Japan: Kanehara & Co., Ltd., 1997.
13. Fong Y, Fortner JF, Sun RL, Brennan MF, Blumgart LH. Clinical score for predicting recurrence after hepatic resection for metastatic colorectal cancer: analysis of 1001 consecutive cases. *Ann Surg* 1999;230:309-21.
14. Minagawa M, Makuuchi M, Torzilli G, Takayama T, Kawasaki S, Kosuge T, et al. Extension of the frontiers of surgical indications in the treatment of liver metastases from colorectal cancer: long-term results. *Ann Surg* 2000;231:487-9.
15. Matsuda K, Hotta T, Uchiyama K, Tani M, Takifuji K, Yokoyama S, et al. Repeat reduction surgery after an initial hepatectomy for patients with colorectal cancer. *Oncol Rep* 2007;18:189-94.
16. Assumpcao L, Choti MA, Gleisner AL, Schulick RD, Swartz MS, Herman J, et al. Patterns of recurrence following liver resection for colorectal metastases: effect of primary rectal tumor site. *Arch Surg* 2008;143:743-9.
17. Jong MC, Pulitano C, Ribero D, Strub J, Mentha G, Schlick RD, et al. Rates and patterns of recurrence following curative intent surgery for colorectal liver metastases: an international multi-institutional analysis of 1669 patients. *Ann Surg* 2009;250:440-8.
18. Jacquet P, Sugarbaker PH. Clinical research methodologies in diagnosis and staging of patients with peritoneal carcinomatosis. *Cancer Treat Res* 1996;82:359-74.

PubMed

Search

Display Settings: Abstract



Genome Res. 2012 Feb;22(2):208-19. Epub 2011 Dec 7.

## Whole-exome sequencing of human pancreatic cancers and characterization of genomic instability caused by MLH1 haploinsufficiency and complete deficiency.

Wang L, Tsutsumi S, Kawaguchi T, Nagasaki K, Tatsuno K, Yamamoto S, Sang F, Sonoda K, Sugawara M, Saiura A, Hirono S, Yamaue H, Miki Y, Isomura M, Totoki Y, Nagae G, Isagawa T, Ueda H, Murayama-Hosokawa S, Shibata T, Sakamoto H, Kanai Y, Kaneda A, Noda T, Aburatani H.

Genome Science Division, Research Center for Advanced Science and Technology (RCAST), The University of Tokyo, Tokyo 153-8904, Japan;

### Abstract

Whole-exome sequencing (Exome-seq) has been successfully applied in several recent studies. We here sequenced the exomes of 15 pancreatic tumor cell lines and their matched normal samples. We captured 162,073 exons of 16,954 genes and sequenced the targeted regions to a mean coverage of 56-fold. This study identified a total of 1517 somatic mutations and validated 934 mutations by transcriptome sequencing. We detected recurrent mutations in 56 genes. Among them, 41 have not been described. The mutation rates varied widely among cell lines. The diversity of the mutation rates was significantly correlated with the distinct MLH1 copy-number status. Exome-seq revealed intensive genomic instability in a cell line with MLH1 homozygous deletion, indicated by a dramatically elevated rate of somatic substitutions, small insertions/deletions (indels), as well as indels in microsatellites. Notably, we found that MLH1 expression was decreased by nearly half in cell lines with an allelic loss of MLH1. While these cell lines were negative in conventional microsatellite instability assay, they showed a 10.5-fold increase in the rate of somatic indels, e.g., truncating indels in TP53 and TGFBR2, indicating MLH1 haploinsufficiency in the correction of DNA indel errors. We further analyzed the exomes of 15 renal cell carcinomas and confirmed MLH1 haploinsufficiency. We observed a much higher rate of indel mutations in the affected cases and identified recurrent truncating indels in several cancer genes such as VHL, PBRM1, and JARID1C. Together, our data suggest that MLH1 hemizygous deletion, through increasing the rate of indel mutations, could drive the development and progression of sporadic cancers.

PMID: 22156295 [PubMed - in process]

**LinkOut - more resources**

PubMed

Search

Display Settings: Abstract



[J Hepatobiliary Pancreat Sci.](#) 2012 Mar;19(2):95-9.

## **Pancreatic dissection in the procedure of pancreaticoduodenectomy (with videos).**

[Yamaue H](#), [Tani M](#), [Kawai M](#), [Hirono S](#), [Okada K](#), [Miyazawa M](#).

Second Department of Surgery, Wakayama Medical University, Wakayama, Japan, [yamaue-h@wakayama-med.ac.jp](mailto:yamaue-h@wakayama-med.ac.jp).

### **Abstract**

The procedure of pancreaticoduodenectomy consists of three parts: resection, lymph node dissection, and reconstruction. A transection of the pancreas is commonly performed after a maneuver of the pancreatic head, exposing of the portal vein or lymph node dissection, and it should be confirmed as a safe method for pancreatic transection for decreasing the incidence of pancreatic fistula. However, there are only a few clinical trials with high levels of evidence for pancreatic surgery. In this report, we discuss the following issues: dissection of peripancreatic tissue, exposing the portal vein, pancreatic transection, dissection of the right hemicircle of the peri-superior mesenteric artery including plexus and lymph nodes, and dissection of the pancreatic parenchyma.

PMID: 22076671 [PubMed - in process]

**LinkOut - more resources**



PubMed



Display Settings: Abstract

Wolters Kluwer | Lippincott  
Williams & Wilkins

[Pharmacogenet Genomics](#). 2012 Jan 29. [Epub ahead of print]

## A genome-wide association study identifies four genetic markers for hematological toxicities in cancer patients receiving gemcitabine therapy.

Kiyotani K, Uno S, Mushiroda T, Takahashi A, Kubo M, Mitsuhashi N, Ina S, Kihara C, Kimura Y, Yamaue H, Hirata K, Nakamura Y, Zembutsu H.

aLaboratory for Pharmacogenetics bLaboratory for Statistical Analysis cLaboratory for Genotyping Development, RIKEN Center for Genomic Medicine, Yokohama dLaboratory of Molecular Medicine, Human Genome Center, Institute of Medical Science, The University of Tokyo, Tokyo eKure Kyosai Hospital, Hiroshima fSecond Department of Surgery, Wakayama Medical University, Wakayama gFirst Department of Surgery, Sapporo Medical University, Sapporo, Japan.

### Abstract

**OBJECTIVE:** Genetic factors are thought to be one of the causes of individual variability in the adverse reactions observed in cancer patients who received gemcitabine therapy. However, genetic factors determining the risk of adverse reactions of gemcitabine are not fully understood.

**PATIENTS AND METHODS:** To identify a genetic factor(s) determining the risk of gemcitabine-induced leukopenia/neutropenia, we conducted a genome-wide association study, by genotyping over 610 000 single nucleotide polymorphisms (SNPs), and a replication study in a total of 174 patients, including 54 patients with at least grade 3 leukopenia/neutropenia and 120 patients without any toxicities.

**RESULTS:** We identified four loci possibly associated with gemcitabine-induced leukopenia/neutropenia [rs11141915 in DAPK1 on chromosome 9q21, combined  $P=1.27 \times 10^{-6}$ , odds ratio (OR)=4.10; rs1901440 on chromosome 2q12, combined  $P=3.11 \times 10^{-6}$ , OR=34.00; rs12046844 in PDE4B on chromosome 1p31, combined  $P=4.56 \times 10^{-6}$ , OR=4.13; rs11719165 on chromosome 3q29, combined  $P=5.98 \times 10^{-6}$ , OR=2.60]. When we examined the combined effects of these four SNPs, by classifying patients into four groups on the basis of the total number of risk genotypes of these four SNPs, significantly higher risks of gemcitabine-induced leukopenia/neutropenia were observed in the patients having two and three risk genotypes ( $P=6.25 \times 10^{-6}$ , OR=11.97 and  $P=4.13 \times 10^{-6}$ , OR=50.00, respectively) relative to patients with zero or one risk genotype.

**CONCLUSION:** We identified four novel SNPs associated with gemcitabine-induced severe leukopenia/neutropenia. These SNPs might be applicable in predicting the risk of hematological toxicity in patients receiving gemcitabine therapy.

PMID: 22293537 [PubMed - as supplied by publisher]

### LinkOut - more resources

#### Full Text Sources

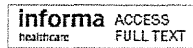
[Lippincott Williams & Wilkins](#)

[Swets Information Services](#)

PubMed



Display Settings: Abstract



[Expert Opin Drug Deliv.](#) 2012 Jan 11. [Epub ahead of print]

## S-1 as a core anticancer fluoropyrimidine agent.

Miura K, Shirasaka T, Yamaue H, Sasaki I.

Tohoku University Graduate School of Medicine, Department of Surgery, 1-1 Seiryomachi, Aoba-ku, Sendai, Miyagi 980-8574, Japan +81227177205; +81227177209; k-miura@surg1.med.tohoku.ac.jp.

### Abstract

**Introduction:** 5-FU is a core anticancer agent for GI and other malignancies, and infusional 5-FU regimens have been widely utilized. Orally administrable fluoropyrimidine prodrugs have been developed to enhance the anticancer efficacy of 5-FU and to reduce its adverse reactions. **Areas covered:** S-1 is an FT-based oral 5-FU prodrug in combination with a DPD inhibitor (CDHP) and an OPRT inhibitor (Oxo), which exerts the following effects: i) maintaining normal gut immunity, Oxo can decrease GI toxicities of 5-FU; ii) sustaining high plasma 5-FU concentrations, Cmax of FBAL after S-1 administration is extremely low, which dramatically decreases adverse reactions such as HFS, neurotoxicities and cardiotoxicities; iii) plasma 5-FU concentrations vary less extensively after S-1 administration and iv) S-1 can be safely administered to patients with DPD deficiency. Furthermore, the alternate-day S-1 administration can reduce the GI toxicities and myelotoxicities of 5-FU without reducing its anticancer efficacy, enabling patients to continue the oral administration for 6 - 12 months. **Expert opinion:** Replacement of regimens with infusional 5-FU and other fluoropyrimidines by the alternate-day S-1 administration may be recommended because the latter procedure is efficient for patients while sustaining the enhanced anticancer efficacy of 5-FU and without reducing its dose intensity.

PMID: 22235991 [PubMed - as supplied by publisher]

**LinkOut - more resources**

# Coexpression of MUC16 and mesothelin is related to the invasion process in pancreatic ductal adenocarcinoma

Atsushi Shimizu,<sup>1</sup> Seiko Hirono,<sup>1,4</sup> Masaji Tani,<sup>1</sup> Manabu Kawai,<sup>1</sup> Ken-Ichi Okada,<sup>1</sup> Motoki Miyazawa,<sup>1</sup> Yuji Kitahata,<sup>1</sup> Yasushi Nakamura,<sup>2</sup> Tetsuo Noda,<sup>3</sup> Shozo Yokoyama<sup>1</sup> and Hiroki Yamaue<sup>1</sup>

<sup>1</sup>Second Department of Surgery; <sup>2</sup>Department of Clinical Laboratory Medicine, Wakayama Medical University, Wakayama; <sup>3</sup>Cancer Institute, Japanese Foundation for Cancer Research, Tokyo, Japan

(Received November 18, 2011/Revised December 27, 2011/Accepted December 28, 2011/Accepted manuscript online February 9, 2012)

The invasion process is a crucial step for pancreatic ductal adenocarcinoma (PDAC); however, the genes related to invasion remain unclear. To identify specific genes for the invasion process, we compared microarray data for infiltrating cancer and PanIN-3, which were harvested from an individual PDAC patient by microdissection. Furthermore, immunohistochemical, coimmunoprecipitation and invasion analyses were performed to confirm the biologic significance of molecules identified by expression profile. In the present study, we focused on MUC16 and mesothelin among 87 genes that were significantly upregulated in infiltrating components compared to PanIN-3 in all PDAC patients, because MUC16 was the most differently expressed between two regions, and mesothelin was reported as the receptor for MUC16. Immunohistochemical analysis revealed that MUC16 and mesothelin were expressed simultaneously only in infiltrating components and increased at the invasion front, and binding of MUC16 and mesothelin was found in PDAC by immunoprecipitation assay. The downregulation of MUC16 by shRNA and the blockage of MUC16 binding to mesothelin by antibody inhibited both invasion and migration of pancreatic cancer cell line. MUC16 high/mesothelin high expression was an independent prognostic factor for poor survival in PDAC patients. In conclusion, we identified two specific genes, MUC16 and mesothelin, associated with the invasion process in patients with PDAC. (*Cancer Sci*, doi: 10.1111/j.1349-7006.2012.02214.x, 2012)

For most patients with pancreatic ductal adenocarcinoma (PDAC), the diagnosis is made at an advanced stage,<sup>(1)</sup> the survival rate for these patients is dismal because PDAC has a propensity for early local invasion and vascular dissemination.<sup>(2)</sup> The genetic and biochemical determinants of the process of invasion and metastasis in PDAC are still largely unknown.

Pancreatic ductal adenocarcinoma appears to arise from histologically well-defined precursor lesions in the ducts of the pancreas, called pancreatic intraepithelial neoplasms (PanIN).<sup>(3,4)</sup> PanIN are graded based on their degree of architectural and nuclear atypia and are categorized into a four-tier classification, including PanIN-1A, 1B, 2 and 3.<sup>(5)</sup> PanIN-3 lesions demonstrate widespread loss of nuclear polarity, nuclear atypia and frequent mitoses, and whereas cancerous cells break through the basement membrane, they evolve into infiltrating adenocarcinoma. The invasion process is the crucial step in PDAC because cancer cells that invade the vasculature, or lymphatic or neural vessels, can progress further to metastasis only after obtaining infiltrating status. In the present study, we identified specific molecular markers associated with invasion in PDAC, which might be useful not only as early diagnostic markers but also as new therapeutic targets for patients with PDAC.

Several molecular markers, including tissue plasminogen activator,<sup>(6)</sup> artemin<sup>(7)</sup> and RhoGDI2,<sup>(8)</sup> have been reported to be associated with invasion in PDAC. However, some of these molecular markers are of little clinical value as therapeutic targets for patients with PDAC because these genes are also expressed in normal pancreatic tissues or other normal organs.<sup>(6-8)</sup> In this study, we first used a gene expression profiling technique to identify the specific genes that are differentially expressed between infiltrating cancer cells and PanIN-3 cells, which were harvested from an individual patient by laser microdissection. Based on our gene expression array data, clinical and biologic implications of MUC16 and mesothelin expression were further explored.

## Material and Methods

**Patients.** Our study population included 103 patients with PDAC who underwent curative resection between January 2004 and December 2007 at Wakayama Medical University Hospital (WMUH). Informed consent was obtained from all patients in accordance with the guidelines of the Ethical Committee on Human Research of WMUH. Patient characteristics are presented in Table 1. The TNM staging criteria of the International Union Against Cancer was used for histologic classification.<sup>(9)</sup> None of the patients had received neoadjuvant chemotherapy or radiation therapy before surgery. The median follow-up duration after resection was 16.8 months (range: 1.6-67.3 months).

**Laser microdissection and RNA extraction.** Tissue samples including cancer cells and adjacent normal cells were embedded in Tissue-Tek OCT compound (Sakura Finetek, Torrance, CA, USA) by freezing tissue blocks in liquid nitrogen immediately after surgical resection for expression profiling. We used the tissues obtained from five patients with PDAC who had coexisting infiltrating cancer cells and PanIN-3 cells, and used the tissues from three patients as controls, including two patients with pancreatitis and one patient with bile duct cancer.

The specimens were cut into 9- $\mu$ m sections at  $-20^{\circ}\text{C}$  with the use of a LEICA cryostat (model 3050S; Leica, Tokyo, Japan) and then fixed on slides in 70% ethanol and stained with hematoxylin. The infiltrating cancer cells and PanIN-3 cells were harvested separately from an individual PDAC tissue using laser microdissection. As a control, the normal pancreatic duct cells were also obtained by laser microdissection, because PDAC originates from pancreatic ductal epithelial cells. Before laser microdissection, two pathologists (YS and

<sup>4</sup>To whom correspondence should be addressed.  
E-mail: seiko-h@wakayama-med.ac.jp

**Table 1. Patient characteristics (n = 103)**

Age, median (range)	69 (31–87)
Gender, male/female	54/49
Tumor site, Ph/Pbt/Phbt	71/30/2
Surgical technique, PD/DP/TP	71/30/2
Differentiation, well/moderate/poor	42/51/10
Tumor size	
≤ 20mm	18
>20 but ≤ 40mm	69
>40 but ≤ 60mm	14
>60mm	2
UICC stage	3
IA	3
IB	5
IIA	24
IIB	63
III	1
IV	7
Postoperative recurrence, yes/no	79/24

DP, distal pancreatectomy; Pbt, pancreatic body and tail; PD, pancreatoduodenectomy; Ph, pancreatic head; TP, total pancreatectomy; UICC, Union for International Cancer Control.

YN) diagnosed infiltrating cancer regions and PanIN-3 regions in the PDAC tissues, and normal pancreatic epithelium in normal pancreatic tissues. We estimated that the proportion of infiltrating cancer cells, PanIN-3 cells, or normal pancreatic ductal cells in the laser microdissected purified samples was at least 95%. Hence, we required more than 30 specimens (range, 35–78 specimens) in each sample for infiltrating cancer cells, more than 110 specimens (range, 111–414 specimens) for PanIN-3 cells and more than 450 specimens (range, 450–520 specimens) for normal pancreatic ductal epithelium cells to obtain enough RNA volume to use for our expression analysis. Total RNA was extracted from the harvested cells using the RNeasy Micro Kit (Qiagen, Hilden, Germany). The concentration of each total RNA sample was measured with a Nanodrop ND-1000 spectrophotometer (Nanodrop Technologies, Wilmington, DE, USA). The integrity of the RNA was determined by capillary electrophoresis using an Agilent 2100 Bioanalyzer (Agilent, Santa Clara, CA, USA) and the extracted RNA was accepted for experiments if the RNA integrity reading was >7.0.

**Genome-wide transcriptional profiling.** The gene expression was analyzed with Human Genome U133 Plus 2.0 GeneChips (Affymetrix, Santa Clara, CA, USA). The manufacturer's instructions regarding the protocols and the use of reagents for hybridization, washing and staining were followed (as previously described).<sup>(10)</sup> Data were collected using an Affymetrix GeneChip Scanner 3000 instrument. The cell intensity data files were obtained using the Affymetrix Suite 5.0 software program; then, the array data were imported into a DNA-Chip Analyzer (dChip, <http://www.dchip.org>) for high-level analysis.

**Immunohistochemistry.** Pretreatment was performed in a microwave using citrate buffer (pH 6.0) for 5 × 3 min at 700 W. Endogenous peroxidase activity was blocked with 3% hydrogen peroxide in methanol, and nonspecific binding sites were blocked with 10% normal goat serum. Primary antibodies were diluted in PBS: MUC16 (1:1000, mouse monoclonal, X325, Abcam, Cambridge, UK) and mesothelin (1:20, mouse monoclonal, 5B2, Novacastra, Newcastle upon Tyne, UK). Diluted primary antibodies were added, and samples were incubated overnight at 4°C. Antibody binding was then immunodetected using the avidin–biotin–peroxidase complex, as described by the supplier (Nichirei, Tokyo, Japan). Finally, the

reaction products were demonstrated using a DAB substrate, and then counterstained with hematoxylin, dehydrated with ethanol and fixed with xylene.

To investigate the localization of the MUC16 and mesothelin, fluorescence immunohistochemistry was performed for paraffin-embedded tissue slides. Double labeling of the two mouse monoclonal antibodies (MUC16 [X325] and mesothelin [5B2]) was done using a Zenon kit (Molecular Probes, Eugene, OR, USA) to directly label the antibodies with either Alexa Fluor 488 or 594 according to the manufacturer's instructions.

**Evaluation of immunohistochemistry.** For scoring assessment, 200 cells were counted in each of the five different fields with high magnification, ×400, on the maximum cut surface of the tumor. We used ovarian cancer tissue and mesothelioma tissue as positive controls for MUC16 and mesothelin expression, respectively. The staining intensity was defined as follows: 0, no staining; 1+, weak; 2+, moderate; 3+, strong, based on the intensity levels of positive control being taken as 3+ (Fig. 1A).<sup>(11–13)</sup> If there were areas with a variety of staining intensities, the predominant intensity was chosen. The quantification of positivity (0–100%) was based on an estimate of the percentage of stained cancer cells in the lesion. The final immunostaining scores were calculated by multiplying the staining intensity and percentage positivity, thereby giving immunostaining scores ranging from 0 to 300.<sup>(14–17)</sup> The cut-off values of immunostaining scores were set as the median value, in accordance with previous reports.<sup>(18,19)</sup> The immunostains were scored by three investigators (SH, YN and HY) blinded to the clinical and pathologic data. If differences of opinion arose, a consensus was achieved by discussion.

**Cell lines and RNA interference.** Human pancreatic cancer cell line PK9 was obtained from the Cell Resource Center for Biomedical Research Institute of Development, Tohoku University (Miyagi, Japan).

Short hairpin RNA (shRNA) plasmids designed to target MUC16 were synthesized by SA Biosciences (Frederick, MD, USA) as follows: insert sequence ACAGCAGCATCAAGA-GTTATT and ggaatctcattcgatgcatac (negative control). Each plasmid (0.8 μg) was mixed with 1 μL Lipofectamine2000 (Invitrogen, Carlsbad, CA, USA) in a final volume of 100 μL of Opti-MEM medium and was added to PK9 cells grown to 40% confluence in 24-well plates. Forty-eight hours after transfection, G418 solution (Roche, Basel, Switzerland) was added in the appropriate concentration. The stably transfected cells were maintained in RPMI-1640.

**Coimmunoprecipitation assay.** To address binding between MUC16 and mesothelin, we performed coimmunoprecipitation assays using pancreatic cancer cell line PK9 and two surgical specimens obtained from 2 PDAC patients. The coimmunoprecipitation assays were performed using the Universal Magnetic Co-IP Kit (Active Motif, Rixensart, Belgium) according to the manufacturer's protocol. Monoclonal antibody against CA125 (OC125, Abcam, Cambridge, UK), monoclonal antibody against mesothelin (MN-1, Rockland, Gilbertsville, PA, USA) or rabbit IgG control (Abcam) were used for immunoprecipitation and immunoblotting.

**In vitro invasion and migration assay in PK9 cell line transfected with MUC16 shRNA.** To investigate the effect of MUC16 expression on invasion and migration of pancreatic cancer cells, *in vitro* invasion and migration assays were performed in the membrane culture system using an 8-μm pore size PET membrane coated with or without Matrigel (24-well, BD Biosciences, San Diego, CA, USA). Parental PK9 cells, vector control-PK9 cells and PK9 cells transfected with MUC16 shRNA were seeded into 5 × 10<sup>4</sup> cells/500 μL growth medium on the Matrigel layer. The following procedures were performed (as previously described).<sup>(20)</sup>

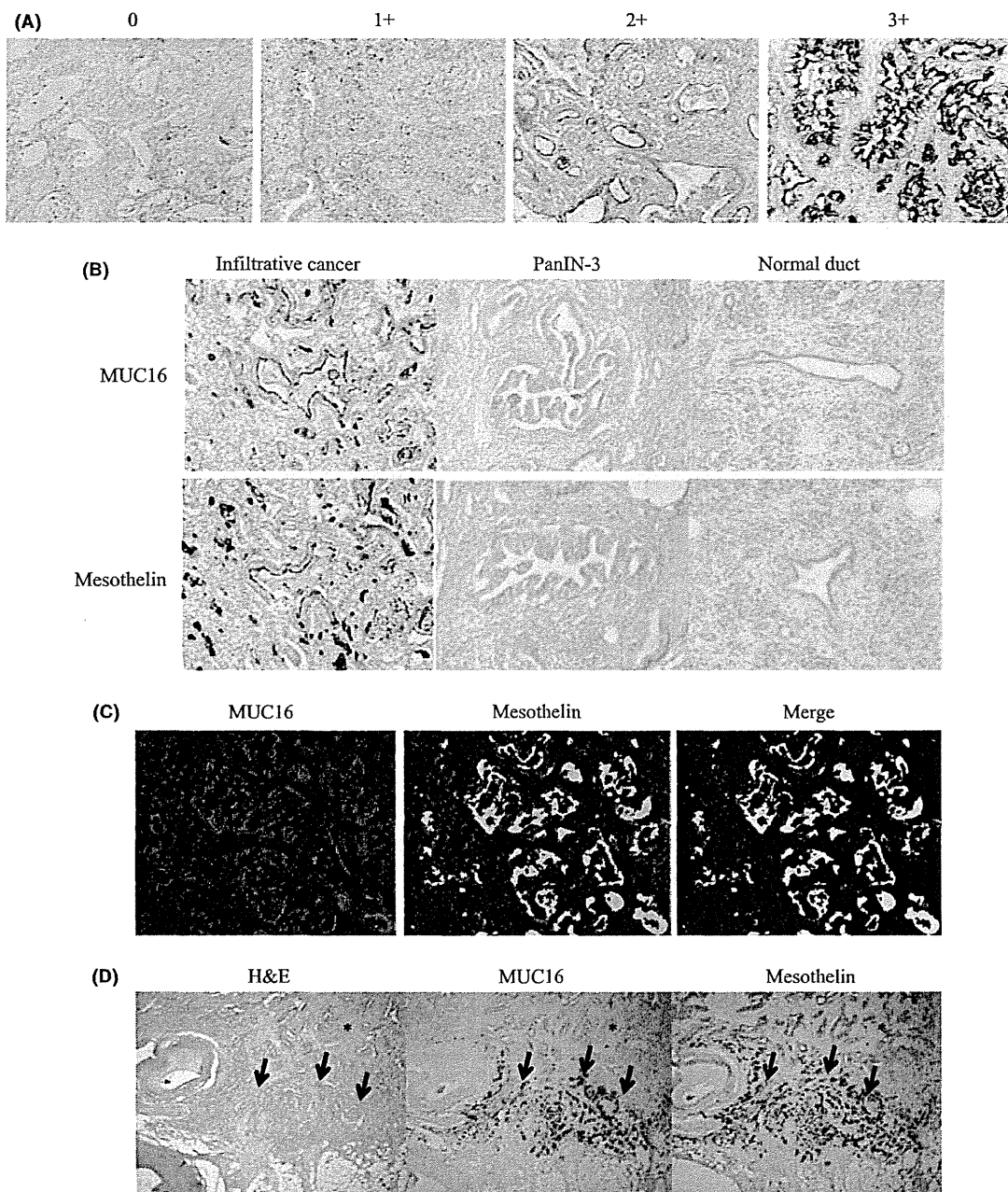


**Fig. 1.** (A) Image of staining intensity grade. (0) no staining, (1+) weak, (2+) moderate, (3+) strong intensity. (B) MUC16 and mesothelin were stained at the apical membrane or cytoplasm only in infiltrative cancer, whereas no staining appeared in PanIN-3 cells and normal ductal cells. (C) MUC16 and mesothelin expressed at the apical cancer cell surface in invasive ductal cancer cells labeled with Zenon Alexa Fluor 594 and 488. The merged image shows MUC16 and mesothelin expressed in the same cancer cells simultaneously. (D) The expression of MUC16 and mesothelin was higher at the invasion front (arrow) than in the main tumor (\*). H&E, hematoxylin and eosin stain.

***In vitro* invasion and migration assays with blocking antibodies for MUC16 and mesothelin.** To investigate the binding between MUC16 and mesothelin, we evaluated the effect of blocking antibodies against interaction between MUC16 and mesothelin on invasion and migration of pancreatic cancer cell PK9 by using *in vitro* invasion and migration assay. Because OC125 (DAKO, Carpinteria, CA, USA) and M11 (DAKO) are known to block the interaction between MUC16 and mesothelin,<sup>(21)</sup> each antibody was used for blocking the interaction. Sodium azide was removed using the AbSelect Antibody Purification System (Innova Biosciences, Cambridge, UK).

**Statistical analysis.** The association between MUC16/mesothelin expression and clinicopathologic factors in the patients with PDAC was assessed using the  $\chi^2$ -test or the Fisher exact test. The survival curves were calculated using the Kaplan–Meier method and then compared by means of the log-rank test. The prognostic significance of clinicopathologic features and MUC16/mesothelin expression was determined using univariate Cox regression analysis. Cox proportional hazards models were fitted for multivariate analysis. Statistical procedures were performed using SPSS version 13.0 (SPSS, Chicago, IL, USA).  $P < 0.05$  was considered statistically significant.

## Results

**Identification of the transcriptional biomarkers associated with the invasion of pancreatic ductal adenocarcinoma by gene expression profiling.** Microarray data for the infiltrating cancer and PanIN-3, which were harvested from an individual PDAC patient, were compared on the basis of the following criteria: (i) a  $\geq 1.5$ -fold change in the expression levels between the infiltrating cells and PanIN-3 cells; (ii) a  $>100$  absolute difference between the expression levels of the infiltrating cells and PanIN-3 cells; and (iii)  $P < 0.05$ .<sup>(22,23)</sup> A total of 109 genes were differentially expressed between infiltrating cancer and PanIN-3 cells in PDAC, including 87 genes that were upregulated and 22 that were downregulated in the infiltrating PDAC, and then 18 genes, which were expressed more in both infiltrating cancer and PanIN-3 than in normal pancreatic epithelium, were listed (see Table 2), to focus on more significant genes related to carcinogenesis in PDAC. Among the upregulated genes identified by expression profiling, we focused on MUC16 because MUC16 expression in the infiltrating cancer was substantially higher than that of the PanIN-3 cells in all five PDAC patients and normal pancreatic duct epithelium (Table 2), indicating that MUC16 is specifically expressed in invasive PDAC. We also focused on mesothelin in the upregulated genes list, because it had been previously reported to be a ligand receptor of MUC16.<sup>(24,25)</sup>

**Immunohistochemical staining of MUC16 and mesothelin in pancreatic ductal adenocarcinoma.** The immunohistochemical analyses were performed in the paraffin-embedded tissues from 103 patients with PDAC. MUC16 and mesothelin were stained by immunohistochemistry at the tumor apical membrane or cytoplasm (or both) in PDAC samples (Fig. 1B). Both MUC16 and mesothelin were expressed only in the infiltrating cancer cells and not in the PanIN-3 cells ( $n = 30$ ) or normal pancreatic epithelial cells ( $n = 103$ ) (Fig. 1B). Furthermore, we found that these genes were not expressed in any non-epithelial cells, including stromal cells, acinar cells and islet cells. Fluorescence immunohistochemistry using the merge technique showed that MUC16 and mesothelin were stained in the same cancer cells simultaneously (Fig. 1C). We observed that

MUC16 and mesothelin were more highly expressed at the invasion front than in the main tumor in 48 of the 103 patients (47%) with PDAC (Fig. 1D).

The scores of MUC16 and mesothelin expression were calculated for each sample. The median scores of MUC16 and mesothelin were 150 (range, 0–300) and 180 (range, 0–300), respectively. The binarization of the score data for these markers was performed as “high expression” versus “low expression” at the median level. We categorized all samples into two groups to analyze the association of MUC16 and mesothelin expression with the clinicopathologic features in the patients with PDAC: the MUC16 high/mesothelin high expression group ( $n = 41$ ) versus the other group ( $n = 62$ ), which included the patients with MUC16 high/mesothelin low expression ( $n = 11$ ), those with MUC16 low/mesothelin high expression ( $n = 11$ ) and MUC16 low/mesothelin low expression ( $n = 40$ ).

**Association of MUC16 and mesothelin expression with pathologic factors.** The correlation of pathologic factors and MUC16/mesothelin expression was analyzed (Table 3). These pathologic factors were evaluated in accordance with the second English edition of the Classification of Pancreatic Carcinoma, proposed by the Japan Pancreas Society.<sup>(26)</sup> The analysis indicated that a tumor size  $>4.0$  cm, serosal invasion, invasion of other organs, and lymphatic permeation occurred significantly more often in the MUC16 high/mesothelin high expression group than in the other groups ( $P = 0.0041$ ,  $P = 0.0131$ ,  $P = 0.0356$  and  $P = 0.0250$ , respectively).

**Binding of MUC16 and mesothelin in pancreatic cancer cell PK9 and surgical specimens from patients with pancreatic ductal adenocarcinoma.** The coimmunoprecipitation assays between MUC16 and mesothelin using pancreatic cancer cell line PK9 and surgical specimens obtained from two PDAC patients (number 1: stage IIB, number 2: stage IV) showed that the whole cell lysates or tissue homogenates were immunoprecipitated and immunoblotted with anti-MUC16 and anti-mesothelin antibody (Fig. 2A), indicating that MUC16 and mesothelin can bind in PDAC.

**Role of MUC16 and mesothelin in invasion, migration and cell growth of pancreatic cancer cell line.** PK9 cells express MUC16 and were transfected with shRNA targeted to MUC16. Stable

**Table 2. Upregulated genes in the infiltrating cancer compared to PanIN-3 component of pancreatic ductal adenocarcinoma as determined by expression profiling**

Probe ID	Gene name	Gene symbol	Fold change, mean	Mean expression level	
				IC/PanIN-3	IC/normal
220196_at	Mucin 16	MUC16	26.7	14.6	31.6
206884_s_at	Sciellin	SCEL	17.4	3.8	4.7
205388_at	Troponin C type 2	TNNC2	10.1	4.1	10.0
204416_x_at	Apolipoprotein C-1	APOC1	6.7	5.9	7.2
213524_s_at	G0/G1switch 2	G0S2	5.4	4.3	13.9
202504_at	Tripartite motif-containing 29	TRIM29	4.5	2.6	8.8
204070_at	Retinoic acid receptor responder 3	RARRES3	3.7	3.4	5.4
242625_at	Radical S-adenosyl methionine domain containing 2	RSAD2	3.6	2.4	12.1
204885_s_at	Mesothelin	MSLN	3.0	2.2	2.2
201564_s_at	Fascin homolog 1, actin-bundling protein	FSCN1	3.0	2.7	3.1
205483_s_at	Interferon, alpha-inducible protein	IFI	3.0	2.5	7.6
228640_at	BH-protocadherin	PCDH7	2.7	2.5	7.5
239979_at	Epithelial stromal interaction 1	EPST1	2.5	2.1	6.5
231956_at	KIAA1618	KIAA1618	2.4	2.4	3.8
204285_s_at	Phorbol-12-myristate-13-acetate-induced protein 1	PMAIP1	2.2	2.1	3.4
222810_s_at	RAS protein activator like 2	RASAL2	2.2	2.2	2.3
243271_at	Sterile alpha motif domain containing 9-like	SAMD9L	2.1	1.9	5.7
200736_s_at	Glutathione peroxidase 1	GPX1	2.0	1.9	2.0

IC, infiltrating cancer; PanIN, pancreatic intraepithelial neoplasms.

**Table 3. The association of MUC16 and mesothelin expression with pathologic factors in patients with pancreatic ductal adenocarcinoma**

	Number	MUC16 high/ mesothelin high group	Other group	P
		41	62	
<b>Differentiation</b>				
Well/ moderate	93	35	57	0.1908
Poor	10	6	4	
<b>Tumor size</b>				
>40mm	16	12	4	0.0041
≤ 40mm	87	29	58	
<b>Local progression</b>				
<b>Intrapancreatic common bile duct invasion</b>				
Positive	22	6	16	0.1757
Negative	81	35	46	
<b>Duodenal invasion</b>				
Positive	40	12	28	0.1052
Negative	63	29	34	
<b>Serosal invasion</b>				
Positive	74	35	39	0.0131
Negative	29	6	23	
<b>Retropancreatic tissue invasion</b>				
Positive	85	35	50	0.5369
Negative	18	6	12	
<b>Portal venous system invasion</b>				
Positive	25	13	12	0.1523
Negative	78	28	50	
<b>Arterial system invasion</b>				
Positive	5	4	1	0.0803
Negative	98	37	61	
<b>Extrapancreatic nerve plexus invasion</b>				
Positive	33	16	17	0.2166
Negative	70	25	45	
<b>Invasion of other organs</b>				
Positive	6	5	1	0.0356
Negative	97	36	61	
<b>Lymphatic permeation</b>				
Positive	88	39	49	0.0250
Negative	15	2	13	
<b>Vascular permeation</b>				
Positive	64	28	36	0.2948
Negative	39	13	26	
<b>Perineural invasion</b>				
Positive	76	29	47	0.5665
Negative	27	12	15	
<b>Lymph node metastasis</b>				
Positive	69	32	37	0.0523
Negative	34	9	25	

MUC16–shRNA-transfected PK9 cells showed downregulation of MUC16 protein expression compared to the vector control (data not shown). Invasion chamber experiments revealed that MUC16–shRNA-transfected PK9 cells had significant suppression of cell invasion (Fig. 2B). Migration assays also demonstrated that downregulation of MUC16 significantly reduced migration (Fig. 2C). The blockage of MUC16 binding to mesothelin with the neutralizing antibodies against MUC16 (OC125 or M11) significantly suppressed invasion and migration of pancreatic cancer cells (Fig. 2D,E). In terms of the effect of MUC16 on cell growth, parental PK9 cells, vector control-PK9 cells and MUC16–shRNA-transfected PK9 were seeded in concentration of  $10 \times 10^4$ /mL, and the cell numbers

were counted on day 1, 3 and 5 using a hemocytometer. As a result, the cell growth was significantly suppressed after inhibition of MUC16 expression (Fig. 2F).

**Association of MUC16 and mesothelin expression with survival in patients with pancreatic ductal adenocarcinoma.** The overall survival of the MUC16 high/mesothelin high expression group was significantly worse than in the other group (median 11.9 vs 22.8 months,  $P = 0.0006$ ; Fig. 3A). The 1-, 3- and 5-year survival rates of the MUC16 high/mesothelin high group versus the other group were as follows: 51.2 vs 72.6%, 8.0 vs 25.6% and 0 vs 11.5%, respectively. The disease-free survival of the MUC16 high/mesothelin high expression group was also worse than the other group (median 6.7 vs 10.9 months,  $P = 0.0002$ ; Fig. 3B). The 1-, 3- and 5-year disease-free survival rates of the MUC16 high/mesothelin high group versus the other group were as follows: 12.2 vs 48.4%, 2.5 vs 20.3% and 0 vs 11.5%, respectively. In the univariate analysis of the overall survival of the patients with PDAC, a tumor size > 4.0 cm, duodenal invasion, portal venous system invasion, lymphatic permeation, vascular permeation, lymph node metastasis and MUC16 high/mesothelin high expression were potential factors for predicting poor survival (Table 4). According to a multivariate analysis of overall survival, vascular permeation and MUC16 high/mesothelin high expression were independent factors for predicting short survival for the patients with PDAC ( $P = 0.0025$ , HR, 2.241; 95% CI, 1.364–4.310;  $P = 0.0158$ , HR, 1.936; 95%CI, 1.132–3.310, respectively; Table 4). Similarly, in the multivariate analysis of disease-free survival, a tumor size > 4.0 cm, lymphatic permeation and MUC16 high/mesothelin high expression were independent prognostic factors for a poorer disease-free survival ( $P = 0.0167$ , HR, 2.141, 95% CI, 1.148–4.000;  $P = 0.0202$ , HR, 3.984, 95% CI, 1.241–12.821;  $P = 0.0131$ , HR, 1.985, 95% CI, 1.155–3.412, respectively; Table 5).

## Discussion

We first identified genes specific to the invasion process in PDAC using microdissection and gene expression profiling techniques. In this study, we compared microarray data of infiltrating cancer and PanIN3, which were harvested from an individual PDAC patient, to exclude the difference in original gene expression among individuals. Then, we were able to identify similar genes that were differently expressed between infiltrating cancer and PanIN-3 in all five patients.

Among the identified upregulated genes, we focused on MUC16 because its expression in the infiltrating cancer was substantially higher than that in the PanIN-3 cells. We also focused on mesothelin in the list, because it was reported to be a ligand receptor of MUC16. Their interaction has been postulated to play an important role during tumorigenesis and metastasis in ovarian cancer.<sup>(24,25)</sup> Rump and colleagues reported that the binding of MUC16 and mesothelin expressed by cancer cells mediates heterotypic cell adhesion and might contribute to the metastasis and invasion of ovarian cancer.<sup>(24)</sup>

In the present study, immunohistochemical analysis revealed that MUC16 and mesothelin were expressed in the infiltrating cancer cells but not in the PanIN-3 cells or normal pancreatic tissues, consistent with the results of gene expression profiling. Furthermore, fluorescence immunohistochemistry showed that MUC16 and mesothelin were expressed simultaneously in the PDAC cells.

MUC16 encodes the CA125 antigen and is a membrane-bound mucin protein with a high molecular weight between 2.5 and 5.0 million daltons.<sup>(27)</sup> Its proposed structure comprises an N-terminal domain of >22 000 amino acid residues that are presumably heavily glycosylated, a central domain containing up to 60 glycosylated repeat sequences constituting

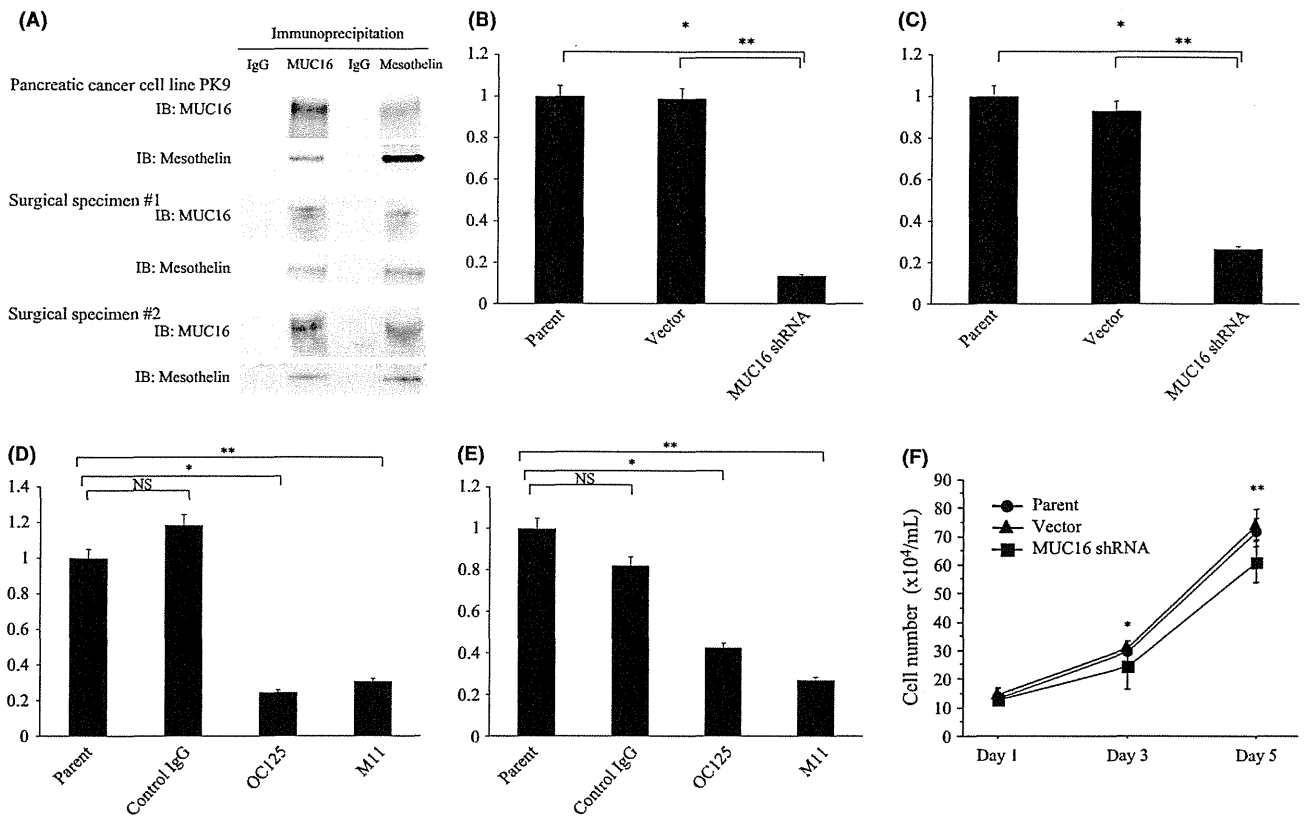


**Fig. 2.** (A) The results of coimmunoprecipitation assay in pancreatic cancer cell line PK9 and clinical samples from the patients with pancreatic ductal adenocarcinoma. The whole cell lysates extracted from cell line or tissue homogenates extracted from two surgical specimens were immunoprecipitated and immunoblotted with anti-MUC16 and anti-mesothelin antibody. IB, immunoblotting. (B) Invasion chamber experiments in PK9 transfected with MUC16 shRNA. The invasion was significantly suppressed after inhibition of MUC16 expression (\* $P = 0.0009$ , \*\* $P = 0.0067$ ). (C) Migration assays in PK9 transfected with MUC16 shRNA. The migration was significantly suppressed after downregulation of MUC16 expression (\* $P = 0.0005$ , \*\* $P = 0.0055$ ). (D) Invasion assay with the blockage of MUC16 binding to mesothelin with the neutralizing antibodies against MUC16 (OC125 or M11, \* $P = 0.0014$ , \*\* $P = 0.0043$ ). (E) Migration assay with the blockage of MUC16 binding to mesothelin with OC125 or M11 (\* $P = 0.0020$ , \*\* $P = 0.0003$ ). (F) Cell growth assay in PK9 transfected with MUC16 shRNA. The cell growth was significantly suppressed after inhibition of MUC16 expression (\* $P = 0.0469$ , \*\* $P = 0.0036$ ). NS, not significant.

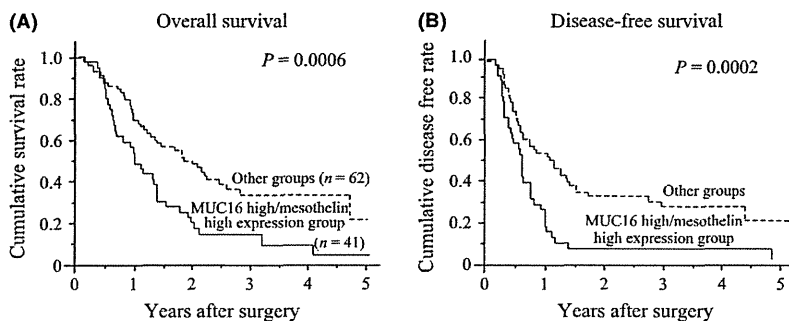


**Fig. 3.** The overall survival (A) and disease-free survival (B) of the MUC16 high/mesothelin high expression group was worse than that of the other groups (median, 11.9 vs 22.8 months,  $P = 0.0006$ ; 6.7 vs 10.9 months,  $P = 0.0002$ , respectively).

the tandem repeats characteristic of mucins, and a C-terminal domain composed of a transmembrane domain and a short cytoplasmic tail with possible phosphorylation sites.<sup>(28)</sup> Few reports have described the expression of MUC16 in cancers. In this study, using immunohistochemistry, we detected the expression of MUC16 in 94 of 103 PDAC cases (91%).

The mesothelin gene encodes a 71-kDa precursor protein that is processed into the 40-kDa glycosylphosphatidylinositol-anchored membrane glycoprotein, mesothelin and a 31-kDa fragment called megakaryocyte potentiating factor.<sup>(29,30)</sup> Mesothelin expression in normal human tissues is limited to mesothelial cells lining the pleura, pericardium and peritoneum,<sup>(29)</sup>

and the protein is also expressed by a variety of solid tumors, including ovarian cancer, malignant mesothelioma, lung cancer and PDAC.<sup>(31,32)</sup> Mesothelin expression reportedly conferred chemoresistance and a poorer clinical outcome in ovarian cancer patients.<sup>(33)</sup>

We found that the coexpression of MUC16 and mesothelin was also increased at the invasion front ( $n = 48$ ), compared to that in the main tumor in several PDAC tissues, and, then, MUC16 high/mesothelin high expression in PDAC was significantly associated with large tumors, serosal invasion, invasion of other organs and lymphatic permeation. These results indicate that these molecules seem to be involved in invasion and



**Table 4. Univariate and multivariate analysis using the Cox proportional hazards regression model of overall survival in 103 patients with pancreatic ductal adenocarcinoma**

	Univariate analysis			Multivariate analysis		
	P	HR	95% CI	P	HR	95% CI
Age, ≥ 70	0.2692	0.906	0.962–1.011	–	–	–
Gender, male	0.7711	1.026	0.678–1.689	–	–	–
Differentiation, poor	0.9228	1.043	0.451–2.410	–	–	–
Tumor size, > 40 mm	0.0070	2.203	1.241–3.906	0.3294	1.340	0.743–2.421
Local progression						
CH, positive	0.1651	1.458	0.856–2.481	–	–	–
DU, positive	0.0465	1.595	1.007–2.525	0.0782	1.575	0.950–2.604
S, positive	0.3320	1.297	0.767–2.188	–	–	–
RP, positive	0.0715	1.848	0.948–3.610	–	–	–
PV, positive	0.0203	1.818	1.098–3.012	0.6830	1.119	0.653–1.916
A, positive	0.6183	1.259	0.507–3.135	–	–	–
PL, positive	0.0666	1.543	0.971–2.451	–	–	–
OO, positive	0.4899	1.342	0.581–3.101	–	–	–
Lymphatic permeation, positive	0.0034	3.937	1.575–9.804	0.1190	2.375	0.801–7.042
Vascular permeation, positive	< 0.0001	3.155	1.859–5.348	0.0025	2.421	1.364–4.310
Perineural invasion, positive	0.1345	1.527	0.877–2.660	–	–	–
Lymph node metastasis, positive	0.0043	2.151	1.272–3.636	0.8436	1.067	0.561–2.033
MUC16/mesothelin expression, high	0.0008	2.206	1.392–3.495	0.0158	1.936	1.132–3.310

A, arterial system invasion; CH, intrapancreatic common bile duct invasion; CI, confidence interval; DU, duodenal invasion; HR, hazard ratio; OO, invasion of other organs; PL, extrapancreatic nerve plexus invasion; PV, portal venous system invasion; RP, retropancreatic tissue invasion; S, serosal invasion.

**Table 5. Univariate and multivariate analysis using the Cox proportional hazards regression model of disease-free survival in 103 patients with pancreatic ductal adenocarcinoma**

	Univariate analysis			Multivariate analysis		
	P	HR	95% CI	P	HR	95% CI
Age, ≥ 70	0.5105	1.161	0.743–1.815	–	–	–
Gender, male	0.9862	0.996	0.638–1.555	–	–	–
Differentiation, poor	0.5830	0.792	0.344–1.825	–	–	–
Tumor size, > 40 mm	0.0001	3.257	1.770–5.988	0.0167	2.141	1.148–4.000
Local progression						
CH, positive	0.6377	1.138	0.664–1.953	–	–	–
DU, positive	0.0105	1.805	1.148–2.833	0.0633	1.590	0.975–2.591
S, positive	0.0864	1.605	0.935–2.755	–	–	–
RP, positive	0.1104	1.689	0.887–3.205	–	–	–
PV, positive	0.0410	1.675	1.021–2.755	0.6492	1.136	0.656–1.965
A, positive	0.8599	1.095	0.397–3.021	–	–	–
PL, positive	0.2523	1.316	0.822–2.110	–	–	–
OO, positive	0.7087	1.189	0.479–2.959	–	–	–
Lymphatic permeation, positive	0.0034	3.937	2.370–18.181	0.0202	3.984	1.241–12.821
Vascular permeation, positive	0.0012	2.198	1.362–3.546	0.1429	1.506	0.871–2.604
Perineural invasion, positive	0.0452	1.736	1.012–2.985	0.1162	1.577	0.894–2.778
Lymph node metastasis, positive	< 0.0001	3.778	1.938–5.917	0.2388	1.484	0.770–2.857
MUC16/mesothelin expression, high	0.0002	2.378	1.497–3.777	0.0131	1.985	1.155–3.412

A, arterial system invasion; CH, intrapancreatic common bile duct invasion; CI, confidence interval; DU, duodenal invasion; HR, hazard ratio; OO, invasion of other organs; PL, extrapancreatic nerve plexus invasion; PV, portal venous system invasion; RP, retropancreatic tissue invasion; S, serosal invasion.

migration of pancreatic cancer cells. Recent reports show the role of MUC16 in ovarian cancer tumorigenesis,<sup>(34,35)</sup> and it has been noted that MUC16 regulates cell growth, invasion and metastasis in epithelial ovarian cancer.<sup>(34)</sup> However, another report indicates the opposite concept, that downregulation of MUC16 inhibits invasion and migration due to the suppression of epithelial to mesenchymal transition in ovarian cancer cells.<sup>(35)</sup> Thus, the role of MUC16 in ovarian cancer cell invasion and migration is still controversial and no report regarding the role of MUC16 on pancreatic cancer cell invasion and migration has yet appeared.

To examine the role of interaction of MUC16 and mesothelin on pancreatic cancer invasion and migration, we investigated whether shRNA and blocking antibodies for MUC16 suppress invasion and migration of pancreatic cancer cells. We investigated the expression of MUC16 and mesothelin by RT-PCR, western blotting and immunocytochemistry in eight pancreatic cancer cell lines (PK9, PANC1, MIAPaCa2, AsPC1, BxPC3, Capan-1, Capan-2 and PK1). By RT-PCR, both MUC16 and mesothelin mRNAs were detected in five cell lines, including PK9, AsPC1, BxPC3, Capan-2 and PK1. Using western blotting and immunocytochemistry, the strongest positive

expressions of both MUC16 and mesothelin were found in PK9. Therefore, in the present study, we used only PK9 cell line for biological experiments. The blockage of the interaction between MUC16 and mesothelin suppressed invasion and migration of pancreatic cancer cells, suggesting that MUC16 binding to mesothelin is important for cell invasion and migration in pancreatic cancer cells.

Furthermore, we focused on the survival of patients with MUC16 high and mesothelin high expression because coexpression of these two genes is obviously correlated to the invasion of PDAC, and MUC16 high/mesothelin high expression was an independent prognostic factor for poor survival. We examined whether there are any differences in survival between the MUC16 high/mesothelin high group and the MUC16 high/mesothelin low group or MUC16 low/mesothelin high group. However, these groups were very small ( $n = 11$ ), and larger groups of patients are necessary for further study.

The mechanism of overexpression of MUC16 and mesothelin in PDAC has not yet been clarified yet. It is also unclear whether the coexpression of MUC16 and mesothelin was coincidental or the increased expression of MUC16 was associated with an upregulation of mesothelin expression. These issues

should be clarified in further studies. Moreover, other molecules in Table 2 besides MUC16 and mesothelin might potentially contribute to the invasion process. In the future, we analyze the roles of other upregulated genes in infiltrating cancer than in PanIN-3 for PDAC patients.

In conclusion, MUC16 and mesothelin are involved in pancreatic cancer cell invasion and migration, and MUC16 and mesothelin clinically represent new prognostic biomarkers for PDAC and might be new therapeutic targets for patients with PDAC, including immunotherapy using a peptide vaccine or monoclonal antibody therapy.

## Acknowledgments

This study was supported by Grant-in-Aid no.19390341 and 22791297 from the Ministry of Education, Culture, Sports, Science and Technology of Japan.

## Disclosure Statement

The authors have no conflict of interest.

## References

- Hidalgo M. Pancreatic cancer. *N Engl J Med* 2010; **362**: 1605–17.
- Dumartin L, Quemener C, Laklai H *et al*. Netrin-1 mediates early events in pancreatic adenocarcinoma progression, acting on tumor and endothelial cells. *Gastroenterology* 2010; **138**: 1595–606.
- Hruban RH, Goggins M, Parsons J, Kern SE. Progression model for pancreatic cancer. *Clin Cancer Res* 2000; **6**: 2969–72.
- Hruban RH, Adsay NV, Albores-Saavedra J *et al*. Pancreatic intraepithelial neoplasia: a new nomenclature and classification system for pancreatic duct lesions. *Am J Surg Pathol* 2001; **25**: 579–86.
- Kern S, Hruban R, Hollingsworth MA *et al*. A white paper: the product of a pancreas cancer think tank. *Cancer Res* 2001; **61**: 4923–32.
- Diaz VM, Hurtado M, Thomson TM, Reventos J, Paciucci R. Specific interaction of tissue-type plasminogen activator (t-PA) with annexin II on the membrane of pancreatic cancer cells activates plasminogen and promotes invasion in vitro. *Gut* 2004; **53**: 993–1000.
- Ceyhan GO, Giese NA, Erkan M *et al*. The neurotrophic factor artemin promotes pancreatic cancer invasion. *Ann Surg* 2006; **244**: 274–81.
- Abiatiari I, DeOliveira T, Kerkadze V *et al*. Consensus transcriptome signature of perineural invasion in pancreatic carcinoma. *Mol Cancer Ther* 2009; **8**: 1494–504.
- Sobin LH, Wittekind CH. *International Union Against Cancer: TNM Classification of Malignant Tumors*, 6th edn. New York, NY: Wiley and Liss, 2002.
- Hirono S, Yamaue H, Hoshikawa Y *et al*. Molecular markers associated with lymph node metastasis in pancreatic ductal adenocarcinoma by genome-wide expression profiling. *Cancer Sci* 2010; **101**: 259–66.
- McClelland RA, Finlay P, Walker KJ *et al*. Automated quantitation of immunocytochemically localized estrogen receptors in human breast cancer. *Cancer Res* 1990; **50**: 3545–50.
- Detre S, Saclani Jotti G, Dowsett M. A “quickscore” method for immunohistochemical semiquantitation: Validation for oestrogen receptor in breast carcinomas. *J Clin Pathol* 1995; **48**: 876–8.
- Allred DC, Harvey JM, Berardo M, Clark GM. Prognostic and predictive factors in breast cancer by immunohistochemical analysis. *Mod Pathol* 1998; **11**: 155–68.
- Campagna D, Cope L, Lakkur SS, Henderson C, Laheru D, Iacobuzio-Donahue CA. Gene expression profiles associated with advanced pancreatic cancer. *Int J Clin Exp Pathol* 2008; **1**: 32–43.
- Fritsche P, Seidler B, Schuler S *et al*. HDAC2 mediates therapeutic resistance of pancreatic cancer cells via the BH3-only protein NOXA. *Gut* 2009; **58**: 1399–409.
- Meinhold-Heerlein I, Stenner-Liewen F, Liewen H *et al*. Expression and potential role of Fas-associated phosphatase-1 in ovarian cancer. *Am J Pathol* 2001; **158**: 1335–44.
- Seethala RR, Gooding WE, Handler PN *et al*. Immunohistochemical analysis of phosphotyrosine signal transducer and activator of transcription 3 and epidermal growth factor receptor autocrine signaling pathways in head and neck cancers and metastatic lymph nodes. *Clin Cancer Res* 2008; **14**: 1303–9.
- Campbell EJ, McDuff E, Tatarov O *et al*. Phosphorylated c-Src in the nucleus is associated with improved patient outcome in ER-positive breast cancer. *Br J Cancer* 2008; **99**: 1769–74.
- Cappia S, Righi L, Mirabelli D *et al*. Prognostic role of osteopontin expression in malignant pleural mesothelioma. *Am J Clin Pathol* 2008; **130**: 58–64.
- Ieda J, Yokoyama S, Tamura K *et al*. Re-expression of CEACAM1 long cytoplasmic domain isoform is associated with invasion and migration of colorectal cancer. *Int J Cancer* 2011; **129**: 1351–61.
- Scholler N, Garvik B, Hayden-Ledbetter M, Kline T, Urban N. Development of a CA125-mesothelin cell adhesion assay as a screening tool for biologics discovery. *Cancer Lett* 2007; **8**: 130–6.
- Gronborg M, Kristiansen TZ, Iwahori A *et al*. Biomarker discovery from pancreatic cancer secretome using a differential proteomic approach. *Mol Cell Proteomics* 2006; **5**: 157–71.
- Yamanaka S, Sunamura M, Furukawa T *et al*. Chromosome 12, frequently deleted in human pancreatic cancer, may encode a tumor-suppressor gene that suppresses angiogenesis. *Lab Invest* 2004; **84**: 1339–51.
- Rump A, Morikawa Y, Tanaka M *et al*. Binding of ovarian cancer antigen CA125/MUC16 to mesothelin mediates cell adhesion. *J Biol Chem* 2004; **279**: 9190–8.
- Gubbels JA, Belisle J, Onda M *et al*. Mesothelin-MUC16 binding is a high affinity, N-glycan dependent interaction that facilitates peritoneal metastasis of ovarian tumors. *Mol Cancer* 2006; **5**: 50.
- Japan Pancreas Society. *Classification of Pancreatic Carcinoma*, 2nd English edn. Tokyo: Kanahara, 2003.
- Yin BW, Lloyd KO. Molecular cloning of the CA125 ovarian cancer antigen: identification as a new mucin, MUC16. *J Biol Chem* 2001; **276**: 27371–5.
- O'Brien TJ, Beard JB, Underwood LJ, Shigemasa K. The CA 125 gene: a newly discovered extension of the glycosylated N-terminal domain doubles the size of this extracellular superstructure. *Tumor Biol* 2002; **23**: 154–69.
- Chang K, Pastan I, Willingham MC. Isolation and characterization of a monoclonal antibody, K1, reactive with ovarian cancers and normal mesothelium. *Int J Cancer* 1992; **50**: 373–81.
- Hassan R, Bera T, Pastan I. Mesothelin: a new target for immunotherapy. *Clin Cancer Res* 2004; **10**(12 Pt 1): 3937–42.
- Ordóñez NG. Application of mesothelin immunostaining in tumor diagnosis. *Am J Surg Pathol* 2003; **27**: 1418–28.
- Argani P, Iacobuzio-Donahue CA, Ryu B *et al*. Mesothelin is overexpressed in the vast majority of ductal adenocarcinomas of the pancreas: identification of a new pancreatic cancer marker by serial analysis of gene expression (SAGE). *Clin Cancer Res* 2001; **7**: 3862–8.
- Cheng WF, Huang CY, Chang MC *et al*. High mesothelin correlates with chemoresistance and poor survival in epithelial ovarian carcinoma. *Br J Cancer* 2009; **100**: 1144–53.
- Thériault C, Pinard M, Comamala M *et al*. MUC16 (CA125) regulates epithelial ovarian cancer cell growth, tumorigenesis and metastasis. *Gynecol Oncol* 2011; **121**: 434–43.
- Comamala M, Pinard M, Thériault C *et al*. Downregulation of cell surface CA125/MUC16 induces epithelial-to-mesenchymal transition and restores EGFR signaling in NIH:OVCAR3 ovarian carcinoma cells. *Br J Cancer* 2011; **104**: 989–99.

# CD44 Variant Regulates Redox Status in Cancer Cells by Stabilizing the xCT Subunit of System xc<sup>-</sup> and Thereby Promotes Tumor Growth

Takatsugu Ishimoto,<sup>1,3</sup> Osamu Nagano,<sup>1,2,\*</sup> Toshifumi Yae,<sup>1</sup> Mayumi Tamada,<sup>1</sup> Takeshi Motohara,<sup>1</sup> Hiroko Oshima,<sup>4</sup> Masanobu Oshima,<sup>4</sup> Tatsuya Ikeda,<sup>5</sup> Rika Asaba,<sup>5</sup> Hideki Yagi,<sup>5</sup> Takashi Masuko,<sup>5</sup> Takatsune Shimizu,<sup>1,2</sup> Tomoki Ishikawa,<sup>1,6</sup> Kazuharu Kai,<sup>1</sup> Eri Takahashi,<sup>1</sup> Yu Imamura,<sup>3</sup> Yoshifumi Baba,<sup>3</sup> Mitsuyo Ohmura,<sup>7</sup> Makoto Suematsu,<sup>7,8</sup> Hideo Baba,<sup>3</sup> and Hideyuki Saya<sup>1,2</sup>

<sup>1</sup>Division of Gene Regulation, Institute for Advanced Medical Research, School of Medicine, Keio University, 35 Shinanomachi, Shinjuku-ku, Tokyo 160-8582, Japan

<sup>2</sup>Core Research for Evolutional Science and Technology (CREST), Japan Science and Technology Agency, Tokyo160-8582, Japan

<sup>3</sup>Department of Gastroenterological Surgery, Graduate School of Medical Science, Kumamoto University, 1-1-1 Honjo, Kumamoto 860-8556, Japan

<sup>4</sup>Division of Genetics, Cancer Research Institute, Kanazawa University, 13-1 Takara-machi, Kanazawa 920-0934, Japan

<sup>5</sup>Cell Biology Laboratory, Department of Pharmaceutical Sciences, School of Pharmacy, Kinki University, 4-1 Kowakae 3-chome, Higashiosaka-shi, Osaka 577-8502, Japan

<sup>6</sup>Kasai R&D Center, Daiichi Sankyo Co. Ltd., 1-16-13 Kitakasai, Edogawa-ku, Tokyo 134-8630, Japan

<sup>7</sup>Department of Biochemistry, School of Medicine, Keio University, 35 Shinanomachi, Shinjuku-ku, Tokyo 160-8582, Japan

<sup>8</sup>ERATO Gas Biology Project, Japan Science and Technology Agency, Tokyo 160-8582, Japan

\*Correspondence: osmna@sb3.so-net.ne.jp

DOI 10.1016/j.ccr.2011.01.038

## SUMMARY

CD44 is an adhesion molecule expressed in cancer stem-like cells. Here, we show that a CD44 variant (CD44v) interacts with xCT, a glutamate-cystine transporter, and controls the intracellular level of reduced glutathione (GSH). Human gastrointestinal cancer cells with a high level of CD44 expression showed an enhanced capacity for GSH synthesis and defense against reactive oxygen species (ROS). Ablation of CD44 induced loss of xCT from the cell surface and suppressed tumor growth in a transgenic mouse model of gastric cancer. It also induced activation of p38<sup>MAPK</sup>, a downstream target of ROS, and expression of the gene for the cell cycle inhibitor p21<sup>CIP1/WAF1</sup>. These findings establish a function for CD44v in regulation of ROS defense and tumor growth.

## INTRODUCTION

CD44, a major adhesion molecule for the extracellular matrix, has been implicated in a wide variety of physiological processes, including leukocyte homing and activation, wound healing, and cell migration, as well as in tumor cell invasion and metastasis (Gunthert et al., 1991; Nagano and Saya, 2004; Ponta et al., 2003). It exists in numerous isoforms generated through alternative mRNA splicing. Whereas the standard CD44 isoform

(CD44s) is expressed predominantly in hematopoietic cells and normal epithelial cell subsets, variant isoforms (CD44v) with insertions in the membrane-proximal extracellular region are abundant in epithelial-type carcinomas (Tanabe et al., 1993). However, the functional relevance of CD44v in tumor cells remains unclear.

CD44 has recently been identified as one of the cell surface markers associated with cancer stem cells (CSCs) in several types of tumor (Al-Hajj et al., 2003; Collins et al., 2005; Dalerba

### Significance

Cancer stem cells (CSCs) manifest enhanced protection against reactive oxygen species (ROS), rendering them resistant to chemo- or radiotherapy. Here, we show that expression of the CSC marker CD44, in particular that of a variant isoform (CD44v), contributes to ROS defense by promoting the synthesis of reduced glutathione (GSH), a primary intracellular antioxidant. CD44v interacts with and stabilizes xCT, a subunit of a glutamate-cystine transporter, and thereby promotes the uptake of cystine for GSH synthesis. Our findings reveal a role for CD44v in the protection of CSCs from high levels of ROS in the tumor microenvironment. Moreover, they provide a rationale for CD44v-targeted therapy to impair ROS defense in cancer cells and sensitize them to currently available treatments.

et al., 2007). CSCs are malignant cell subsets in hierarchically organized tumors; they are selectively capable of tumor initiation and self-renewal and give rise to the bulk population of nontumorigenic cancer cells through differentiation. Furthermore, we have recently shown that CD44v is heterogeneously expressed in mouse gastric tumors, being highly abundant in proliferative cells and slow-cycling stem-like cells, but not in cells harboring mucin 5AC (MUC5AC) mRNA, a marker of gastric differentiation (Ishimoto et al., 2010). These observations suggested that CD44 might play a role in tumor initiation and the maintenance of cancer cells in addition to its more established functions in cell adhesion and migration. However, function-based evidence to support such a role for CD44 or its variant isoforms has been lacking.

Oxidative stress occurs when production of reactive oxygen species (ROS) exceeds the capacity of the cellular defense system consisting of redox enzymes and other antioxidant molecules. Like normal tissue stem cells, subsets of CSCs in some tumors harbor only low levels of ROS and manifest enhanced mechanisms for protection against ROS-mediated damage, properties that may contribute to tumor resistance to chemo- and radiotherapy (Diehn et al., 2009; Phillips et al., 2006). Reduced glutathione (GSH) is a major cellular metabolite that protects against oxidative and chemical injury and exhibits a variety of other cytoprotective effects. High levels of GSH as well as increased expression of antioxidant enzymes promote cancer cell survival and resistance to anticancer agents (Trachootham et al., 2009). System xc<sup>-</sup> is a cystine-glutamate exchange transporter composed of a light-chain subunit (xCT, SLC7A11) and a heavy-chain subunit (CD98hc, SLC3A2). Expression of xCT at the cell surface is essential for the uptake of cystine required for intracellular GSH synthesis and is, thus, an important determinant of intracellular redox balance (Lo et al., 2008). Cells deficient in xCT or depleted of GSH have recently been found to exhibit p38<sup>MAPK</sup> activation even at low levels of oxidative stress (Chen et al., 2009; Sato et al., 2005), indicating that xCT-mediated cystine transport for GSH synthesis plays a key role in prevention of such stress signaling. Furthermore, xCT has been implicated in the proliferation and multidrug resistance of several types of cancer cells (Chen et al., 2009; Huang et al., 2005; Lo et al., 2008). We carried out this study to determine the function and mechanism of CD44v in controlling redox status in cancer cells through the regulation of xCT-mediated cystine transport.

## RESULTS

### CD44 Expression Correlates with ROS Defense, and CD44 Ablation Activates ROS-p38<sup>MAPK</sup> Signaling in Gastrointestinal Cancer Cells

CD44 is a cell surface marker for CSCs in various tumors, and CSCs manifest low intracellular levels of ROS and enhanced protection against ROS-mediated damage (Diehn et al., 2009). Therefore, we hypothesized that CD44 expression is functionally related to ROS defense in cancer cells. To investigate this hypothesis we examined five human gastrointestinal cancer cell lines that differ in CD44 expression status: three gastric cancer lines (MKN28, AGS, KATOIII); and two colorectal cancer lines (HT29, HCT116). These cells were exposed to 0.5 mM

hydrogen peroxide (H<sub>2</sub>O<sub>2</sub>) as an oxidative stressor for 20 min and then examined by fluorescence microscopy after staining with 2',7'-dichlorofluorescein diacetate (DCFH-DA), a ROS-sensitive fluorescent probe. The hydrolyzed compound DCFH is oxidized to yield dichlorofluorescein (DCF), which is detectable by fluorescence microscopy or flow cytometry (Behl et al., 1994; Suematsu et al., 1992). In contrast to the cell lines (HCT116, HT29, KATOIII) expressing a high level of CD44 (CD44<sup>high</sup>), those negative for CD44 expression (CD44<sup>neg</sup>, MKN28) or expressing CD44 at a low level (CD44<sup>low</sup>, AGS) showed pronounced DCFH-DA staining (Figure 1A). Thus, this result suggested that CD44<sup>high</sup> gastrointestinal cancer cells have a more efficient ROS defense system than do CD44<sup>neg</sup> or CD44<sup>low</sup> cells.

To examine the functional relevance of CD44 expression to ROS defense in CD44<sup>high</sup> cancer cells, we depleted these cell lines of CD44 by RNA interference (RNAi) (Figure 1B). Flow cytometric analysis revealed that HCT116 cells and HT29 cells depleted of CD44 by transfection with a small interfering RNA (siRNA) specific for CD44 mRNA showed a small increase in DCFH-DA staining compared with those transfected with a control siRNA (Figure 1C; see Figure S1A available online). In KATO III cells, which have a higher basal ROS level than other cell lines, CD44 depletion by transfection with a siRNA specific for CD44 mRNA markedly increased DCFH-DA staining compared with those transfected with a control siRNA (Figure S1A). These results suggest that the increase of ROS levels by CD44 ablation depends on cell context and basal ROS levels.

To exclude the differences of cellular redox status and further examine the role of CD44 on ROS defense ability, we exposed the cells to H<sub>2</sub>O<sub>2</sub>. CD44-deficient HCT116 cells manifested a markedly greater increase in DCFH-DA staining after exposure to H<sub>2</sub>O<sub>2</sub> than did those transfected with the control siRNA (Figure 1C). Similar effects of CD44 ablation on H<sub>2</sub>O<sub>2</sub>-induced DCF fluorescence were also observed in the other two CD44<sup>high</sup> cell lines (HT29, KATOIII), although the efficiency of CD44 knock-down differed between the two lines (Figure S1B). These results indicated that CD44 expression contributes to ROS defense in cancer cells.

To investigate further the potential role of CD44 in the cellular response to oxidative stress, we examined the activation of p38<sup>MAPK</sup>, a major target of ROS (Muller, 2009). Depletion of CD44 by RNAi resulted in a marked increase in the phosphorylation (activation) level of p38<sup>MAPK</sup> in HCT116 cells exposed to H<sub>2</sub>O<sub>2</sub> (Figure 1D). The H<sub>2</sub>O<sub>2</sub>-induced p38<sup>MAPK</sup> activation and ROS accumulation in CD44-deficient HCT116 cells were completely inhibited by treatment with *N*-acetylcysteine (NAC) (Figures 1D and 1E). Thus, NAC treatment reversed the oxidative stress phenotype of the CD44-depleted cells. These results suggested that CD44 promotes ROS metabolism in cancer cells and thereby suppresses the activation of ROS-p38<sup>MAPK</sup> signaling.

### CD44<sup>+</sup> Gastric Tumor Cells Show a Low Level of p38<sup>MAPK</sup> Phosphorylation In Vivo

To address the functional relevance of CD44 expression to gastric tumorigenesis, we studied a transgenic mouse model of gastric cancer, the *K19-Wnt1/C2mE* or *Gan* (gastric neoplasia) mouse, in which both Wnt and prostaglandin E<sub>2</sub> signaling pathways are activated in the gastric mucosa (Oshima et al., 2006). These transgenic animals develop large, well-differentiated